Catena 233 (2023) 107524

Contents lists available at ScienceDirect

Catena

journal homepage: www.elsevier.com/locate/catena

Fate and migration of enhanced rock weathering products through soil horizons; implications of irrigation and percolation regimes

Reza Khalidy, Yi Wai Chiang, Rafael M. Santos *

School of Engineering, University of Guelph, Guelph, Ontario N1G 2W1, Canada

ARTICLE INFO

Keywords:
Enhanced rock weathering
Pedogenic carbonate
Carbon dioxide removal
Negative emissions

ABSTRACT

Terrestrial enhanced rock weathering (ERW) is reckoned as a robust method to contribute to stabilizing atmospheric carbon and combat global warming. The method is particularly a matter of interest in agricultural soil, offering a vast opportunity for the application of crushed silicate minerals and secondary carbonate accumulation and migration. Although the applicability of this practice is well acknowledged, its impact on the geochemical alteration of soil vertical profile, particularly deeper layers, is less discussed in the literature. Moreover, the effect of irrigation and percolation regimes, as influenced by ambient conditions, is also not well-reported and characterized. In the present study, we utilized a high amendment rate (50 t/ha) of wollastonite skarn, a fast-weathering silicate mineral, to uncover the alterations in topsoil and subsoil as well as effluent water over a through a soil column experiment over five months, under more controlled (indoor) and less controlled (outdoor) ambient and irrigation conditions. The results indicate more conspicuous modification of parameters in shallow layers of soil compared to deeper ones, explicitly in the rain-fed setup. Silicate amendment induced an increase of 6.53 and 2.85 tCO_2/ha (in the form of pedogenic carbonate (PC)) over the profile of soil (0–60 cm) under periodic and rain-fed water regimes, respectively. The silicate treatment was also found to be effective toward rising pH and electrical conductivity of topsoil (0–15 and 15–30 cm layers) and leachate, and a measurably greater release of Ca^{2+} and Mg^{2+} in the column effluent. We estimate a carbon drawdown ratio (carbonate/bicarbonate) of ≈15:1 in this study, showing that PC formation is a more significant weathering indicator than leachate bicarbonate export in the shorter term for a fast-weathering mineral in pH-neutral soils and moderate irrigation regime. Such observations are valuable for developing carbon drawdown quantification methods suitable for a variety of agricultural lands and global regions.

1. Introduction

The current upward shifting of atmospheric carbon level due to greenhouse gas emissions could cause severe climatic consequences, including 2° C rise in the Earth's surface temperature (Khalidy and Santos, 2021a; Lindsey and Dahlman, 2020). To harness this trend, several carbon dioxide removal (CDR) approaches have been proposed to sequester carbon in aqueous and terrestrial environments (Gu et al., 2019; Khalidy and Santos, 2021b; Rahmanihanzaki and Hemmati, 2022; Wu et al., 2021). Recently, there has been a tendency toward environmentally benign methods that can stabilize carbon for geological scale timeframes (Kelemen et al., 2020; La Plante et al., 2021; Sanna et al., 2014). Enhanced rock weathering (ERW) is one of these methods that has shown the suitability of carbon capturing in urban (Jorat et al., 2020; Washbourne et al., 2012) and agricultural soils (Haque et al., 2020b; Khalidy et al., 2021) and is deemed as a potential practice for sustainable agriculture (Beerling et al., 2018; Goll et al., 2021; Kantola et al., 2017; Kantzas et al., 2022).

ERW involves the weathering of Mg- and Ca-bearing silicate minerals, occurring naturally in rock formations at a rapid rate (Andrews and Taylor, 2019; Khalidy et al., 2022). The practice of ERW entails a chain of processes beginning with the dissolution of CO_2 in rainwater, followed by the dissolution of the mineral in the soil–water system (Goll et al., 2021; Khalidy et al., 2021). The released cations react with carbonate/bicarbonate and either precipitate as the secondary pedogenic carbonates or find their way to the groundwater system within the flow pathway, both contributing to net carbon uptake and atmospheric CO_2 drawdown (Hartmann et al., 2013; Khalidy et al., 2022).

One concern attributed to this approach is the amount of toxic elements that could be released and migrate downward into groundwater

* Corresponding author.
E-mail address: santosr@uoguelph.ca (R.M. Santos).

https://doi.org/10.1016/j.catena.2023.107524
Received 19 July 2023; Received in revised form 28 August 2023; Accepted 13 September 2023

sources (Dupla et al., 2023; Haque et al., 2020a). This has particularly been reported in the case of olivine (Amann et al., 2020; te Pas et al., 2023), while other ERW candidates (including wollastonite) have exhibited below-regulation levels of concerning metals (Santos et al. 2023). However, it is worth giving attention to this question by assessing toxic metals such as Ni and Cr in experimental/field ERW studies, as mineral feedstocks originate from various sources and some may contain more trace metals than others (Haque et al., 2020a). Another challenge is selecting the appropriate mineral for ERW based on the vicinity of the source of the mineral to the point of application since mining operation and transportation could be costly and energy-consuming (Lefebvre et al., 2019; Moosdorf et al., 2014; Renforth, 2012).

The practice of ERW as a method for capturing atmospheric carbon in the lab (mesocosms in pots, columns, or lysimeters) (Haque et al., 2019; Kelland et al., 2020; Vienne et al., 2022) and field scales (Haque et al., 2020b; Jorat et al., 2022; Khalidy et al., 2021; Manning et al., 2013) is well documented. Focusing on mesocosm-scale, previous studies looked into the impact of Mg-based silicate rocks and minerals (basalt and olivine) on soil and water characteristics (e.g., (Kelland et al., 2020; Renforth et al., 2015; Vienne et al., 2022)). However, investigation of ERW's impact on soil properties with depth is rare and limited in the literature (Renforth et al., 2015). Wollastonite, as a fast-weathering silicate mineral, has shown reliability for CO_2 uptake as well as plant growth in previous studies (Haque et al., 2020c, 2019; Jariwala et al., 2022). Hence, amendment with wollastonite could be advantageous to investigate the accumulation and migration of weathering products over the vertical profile of soil over a relatively short time (e.g., a few months).

In this study, a soil column experiment was developed to study the response of the soil–water system (different layers of soil and effluent water) to the application of crushed wollastonite skarn (a blend of wollastonite with lesser quantities of diopside). The columns were made using distinct layers of soil and subsoil and were exposed to rain-fed and periodic water irrigation regimes in outdoor and indoor settings, respectively, whereby the variations in ambient conditions would regulate percolation through the soil profile. In addition to conventional measurements (carbonate content, pH, and elemental flux), we used mineralogical analyses of X-ray diffraction (XRD) and X-ray fluorescence (XRF) as well as electrical conductivity (EC) measurement as signs of weathering throughout the soil profile.

2. Methods

2.1. Experimental setup

The experimental setups consisted of columns built up of a PVC pipe (60 cm in height, radius = 7.62 cm) and connected to a cap with a hole in the bottom, enabling leachate collection (Fig. S1). The columns were filled with a mildly acidic (pH = 6 ~ 6.5) silt loam (0.6%, 17.3%, 60.3%, and 22.4% by mass of gravel, sand, silt, and clay, respectively) topsoil (0–30 cm) and subsoil (30–60 cm) collected from an agricultural field located in Southwestern Ontario (N 43°07′ W 81°10′). The top- and sub-layer soils were compacted to manage a minimum bulk density of 1350 and 1450 kg/m^3, respectively (no plants were growing in the columns). The top 15 cm layer of "wollastonite amendment" columns was extracted and mixed thoroughly with 90 g of crushed wollastonite skarn (equivalent to 50 t/ha rate), acquired from Rock Powder Solutions Inc. (Canada), before being put back into columns. The characterization of the wollastonite skarn (particle size distribution and elemental composition) and its main mineral phases (through XRD pattern) are shown in Table 1 and Fig. S2, respectively. Based on the elemental composition of wollastonite ore (Table 1) and using stoichiometry, the net amount of wollastonite and diopside in the sample is estimated to be 47.72 g (53.03 wt%) and 19.87 g (22.1 wt%), respectively, with the balance (27.10 wt%) being the sum of other minor phases identified in Fig. S2 that account for the FeO, Na_2O, K_2O and residual SiO_2 content of the mineral. The multipoint Brunauer-Emmett-Teller (BET) surface area and particle size distribution of wollastonite were determined using a physisorption analyzer (Quantachrome Autosorb iQ) and laser diffraction (Malvern Mastersize SM), respectively.

Table 1
Characterization (BET, particle size distribution, and elemental composition) of applied wollastonite.

BET surface area (m^2/g)	0.856 ± 0.01
Particle size (volume %):	
> 500 μm	16.73
250 – 500 μm	33.73
63 – 250 μm	32.16
32 – 63 μm	6.72
< 32 μm	10.59
WDXRF (mass %)	Sum = 99.98 wt%
SiO_2	53.36
TiO_2	0.26
Al_2O_3	3.42
Cr_2O_3	0.03
Fe_2O_3	2.33
MnO	0.04
MgO	4.11
CaO	31.30
SrO	0.23
Na_2O	1.50
K_2O	1.20
P_2O_5	0.20
SO_3	0.96
Cl	0.06
LOI (at 1000 °C)	0.98

Two setups were considered in this study. The first set (two control and two wollastonite amendment columns) was placed in a temperature-controlled (22 ± 3 °C) laboratory throughout the experiment. These columns (termed 'Lab' columns hereafter) were irrigated periodically with 400 ml Milli-Q water with an adjusted pH of 5 ~ 5.5 to emulate rainfall pH. We used a few drops of nitric acid to adjust pH, as nitrate is a plant nutrient commonly found in soils, does not have any negative effect on plants compared to hydrochloric acid, and does not precipitate in the system. The irrigation ran from May to October 2022 (every 4–5 days, for a total of 34 episodes), and the total amount of injected water was equivalent to annual rainfall in Southwestern Ontario, Canada (Government of Canada, 2023).

The other set of columns (two control and two wollastonite amendment columns) was placed on the building rooftop in the School of Engineering, University of Guelph. This set of columns (called 'Rooftop' columns hereafter) was only exposed to rain-fed irrigation during the experiment (June-November 2022). The main objective of running the experiment on a rooftop was to compare how ambient climate conditions (e.g., rainfall, temperature, and evaporation) affect the results compared to the outcome of the Lab setup. To avoid excessive heat transfer and evaporation, the side walls of columns were wrapped with insulation material. Furthermore, the columns were secured in a position that was sheltered from the Sun for at least half of the daytime. It is understood, as discussed by West et al. (2023), that a rooftop location can lead to excessive evapotranspiration compared to local soils, but in the case of the present study, the aim was not necessarily to simulate exact field conditions, but rather to have two sets of columns under different irrigation and temperature cycles to assess how ambient conditions affected wollastonite weathering, leachate collection rate and composition, and pedogenic carbonate formation.

2.2. Soil analyses

After the experiments, the columns were broken, and the soil was split vertically into four pieces of 15 cm (0–15 cm layer as the uppermost and 45–60 cm as the bottommost). The soil samples were air-dried in the lab before further analyses. The pH and EC of soil samples were

determined using a suspension formed by adding a 5:1 volumetric ratio of water to the soil and followed by placing it on a shaker for 1 h. Prior to measurements, the suspension was allowed to settle down for at least one hour (Rayment and Higginson, 1992). The carbonate content of soil samples (soil inorganic carbon (SIC) in $gCaCO_3 \cdot (kg \cdot soil)^{-1}$ was measured by the calcimetry method, as described in Khalidy et al. (2021). Accordingly, 20 ml of MiliQ water was added to soil samples within an Erlenmeyer flask before putting in 7 ml of 4 M HCL. The flask was connected to a graduated water-filled manometer-style column that quantified the released CO_2 volume. The XRD (Panalytical Empyrean) and XRF (Rigaku Supermini 200) were used to identify changes in mineral phases and elemental composition as signs of weathering and transport of wollastonite in soil samples, respectively. Soil organic matter (SOM) was determined using the method of Howard and Howard (1990). Following drying at 105 °C overnight, the samples were combusted at 450 °C for 4 h, recording weight loss as Loss on Ignition (LOI) due to decomposition of organic matter.

2.3. Leachate analyses

The pH and EC of leachate samples were determined using a pH meter (Oakton pH 700 Benchtop meter) and an EC meter (Hanna Instruments), respectively, just after leachate collection.

For the elemental (Ca, Mg, Si, Ni, Cr, and Sr) concentration, the leachate samples were filtered over 0.45 μm syringe filters and 2 vol% acidified by HNO_3 (36 vol%) before storing at 4 °C until analysis with ICP-OES (Varian Vista Pro).

2.4. Data analyses

All readings of experimental analyses on soil and leachate samples were conducted in triplicate, and the mean of results was reported (along with standard error). To discern the statistical significance of treatments (control vs. wollastonite amendment), the Independent Samples T-Test was used in IBM SPSS software.

3. Results and discussion

3.1. Leachate chemistry

We initially aimed to collect leachate from columns set up on the rooftop after each rainfall episode. However, based on our observations, the amount of collected leachate was scarce and insufficient, mainly due to the below-normal rainfall (see Fig. S4) and high evaporation rate due to direct exposure to sunlight. Therefore, only leachate analyses of lab setup are presented here.

The average pH of leachate collected throughout the experiment is demonstrated in Fig. 1. Given the weakly acidic range of irrigation water (pH = 5 ~ 5.5), the elevation of pH to 7 ~ 8 range implies the dissolution of cations in all columns with a pronounced degree in amended columns. These results are in line with some of the data reported in the literature (Amann et al., 2020; Kelland et al., 2020). In contrast, Renforth et al. (2015) and Vienne et al. (2022) did not observe any significant change in the pH of outflow in the case of olivine and basalt amendment, respectively.

Analyses of the elemental budget represent a notable elevation (187 mg on average) of Ca leached in the effluent of amended columns, coming along with a mild upward shift in the case of Mg and Sr (Fig. 1). The other elements (Ni, Cr, and Si) are unlikely to be remarkably affected due to wollastonite amendment.

The evolution of EC variation throughout the experiment in Fig. 2 highlights the depletion of EC gradually over time in samples collected from both control and amended columns. Initially, there is a quite gap between values of control and amended columns, while they tend to draw near over closing stages of the experiment, leaving a roughly insignificant disparity. The higher amount of EC in amended samples

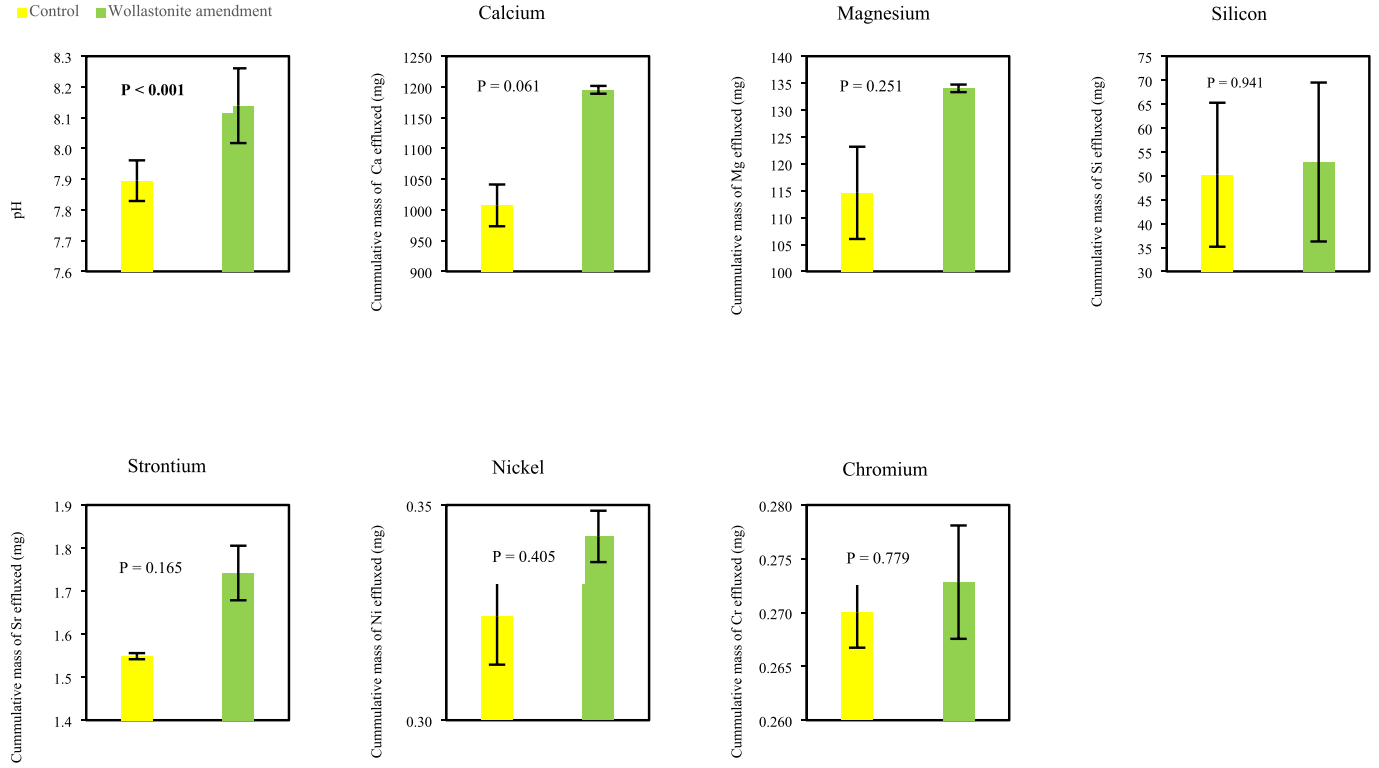

Fig. 1. Impact of wollastonite amendment on biochemistry (pH and elemental budget (by ICP-OES)) of collected leachate. The pH values are means and the elemental values are cumulative masses over the experiment duration (5 months). The method for calculating the cumulative amount of elements is described in the Supplementary Material (Eqs. S1 and S2).

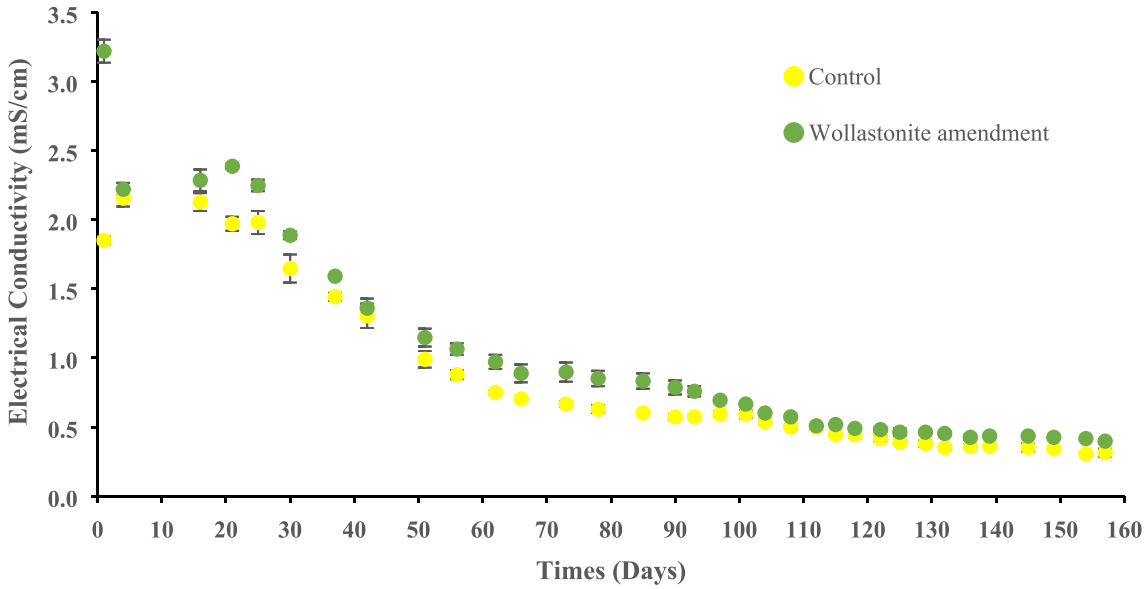

Fig. 2. Analyses of column effluent EC over the course of the experiment; an average of control and amended columns are plotted along with standard errors.

can be deemed as a sign of weathering, as discussed by Amann and Hartmann (2022). However, these authors allude measurement of EC cannot solely account for carbon drawdown in the whole soil–water system, and more robust verification (e.g., multi-parameter analyses) is required, particularly in the groundwater to ocean transport section (Amann and Hartmann, 2022).

3.2. pH and EC of soil

Fig. 3 demonstrates the final pH of soil layers after the experiment. Accordingly, the most evident pH upward shift occurs in the top layer of both Lab (+1.04 unit on average, $P < 0.005$) and Rooftop (+0.41 unit on average, $P < 0.005$). The discrepancy gradually tends to be insignificant toward the bottom layer ($p = 0.384$ and $p = 0.613$ in the Lab and Rooftop, respectively).

Evaluating 12 different land uses in southern China, Yan et al. (2023) deduced a large increment (more than two units) in the pH of the soil (mostly in the strong acidic range) after applying powdered wollastonite. In the study conducted by Kelland et al. (2020), a slight increase of 0.1 unit was observed due to the amendment of soil with basaltic rock

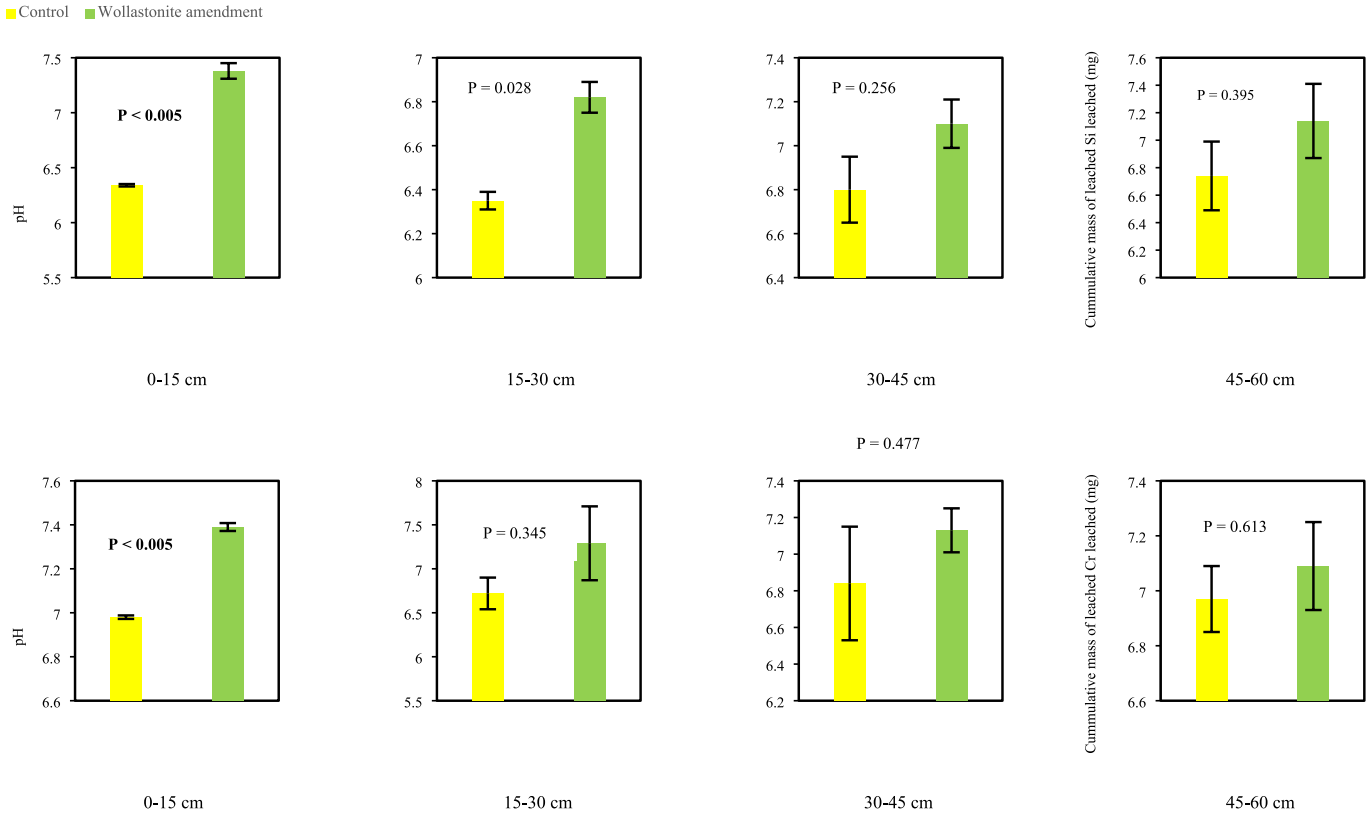

Fig. 3. Impact of wollastonite amendment on pH of different depths over the vertical profile of soil (above: Lab; below: Rooftop).

powder, though the rate of application and pH of native soil were similar to the present study.

The EC of soil layers follows the same trend as of pH over the vertical profile of the soil (Fig. 4) with more than two times increment in upper layers (0–15 and 15–30 cm). We noted that the EC value is higher in rooftop samples compared to corresponding lab samples (the same trend was observed in the pH of surficial layers, Table S1). This could be related to the fact that these columns are subjected to atmospheric dry and wet deposition, adjusting the soil solution EC (Balestrini et al., 2000; Barton et al., 2002).

3.3. Soil carbonate content

As demonstrated in Fig. 5, the amendment with wollastonite brings about accumulation of carbonate in soil, underlining a step up of 3 and 2.5 times on average in carbonate content of the top layer (0–15 cm) of Lab ($P < 0.005$) and Rooftop ($P < 0.05$) setups, respectively. The formation of carbonate is also expanded to the 15–30 cm layer with a lesser degree, but the subsoil layers undergo different trends. In the case of the Lab setup, the 30–45 layer data indicates a large deviation of carbonate measurements and insignificancy ($P = 0.348$), while the bottommost layer shows an increment (around two times) of carbonate content. In contrast, there is a limited augmentation of carbonate content in sublayers of wollastonite amendment columns in the Rooftop setup.

The increase in soil inorganic carbon content due to ERW in mesocosm level was acknowledged by Kelland et al. (2020), while other studies asserted the formation of carbonate is not plausible over a relatively short interval (e.g., a few months) (Renforth et al., 2015; Vienne et al., 2022). Still, both of these studies reported an increase of carbonate content in intermediate layers of their mesocosm (25–50 cm (Vienne et al., 2022) and 50–60 cm (Renforth et al., 2015)). Such discrepancy could emerge from the relatively faster weathering rate of wollastonite compared to other silicate minerals (basalt and olivine) employed in the mentioned studies. The other effective parameters could be regime and amount of irrigated water as well as soil properties (e.g., pH, density, and texture).

3.4. XRD/XRF

Due to the complexity of soil composition, detecting signs of enhanced rock weathering in soil through XRD is burdensome (Haque et al., 2020b). However, this analysis was conducted on samples of the top (0–15 cm) layer samples. The XRD diffractograms of soil mineral phases are shown in Fig. 6 and Fig. S3. Accordingly, the phases of calcite (as a sign of carbonate precipitation), wollastonite, and diopside (as a sign of mineral mixture with soil) are remarked in the amended sample. In addition, quartz, albite, and feldspar are the main phases of soil observed in both control and wollastonite amendment samples.

Fig. 7 shows the difference in key elements composition of top and subsoil samples (considering the difference of control and corresponding wollastonite amendment values). These elements were highlighted as either signature of weathering or abundance in the composition of wollastonite skarn(Table.1). The main remarkable point is the increment of CaO (more than 1%) and MgO (between 0.1 and 1%) in 0–15 cm layer of both Lab and Rooftop setups as well as downward migration and accumulation of Si in 30–45 cm layer. The change in other elements remains insignificant (<0.01%). The same pattern of enrichment in weathering element (Mg) in shallow layers and Si migration in soil vertical profile was reported by Renforth et al. (2015).

3.5. Organic matter

The LOI was conducted to assess the impact of the wollastonite amendment on change in SOM, as it positively correlates with SOC (Ruiz Sinoga et al., 2012). The SOM values over the vertical profile of soil are represented in Fig. 8. The results highlight a slight decrease in SOM due to wollastonite application in surficial layers (0–15 and 15–30 cm in the Lab and 0–15 cm in the Rooftop setups). In contrast, the SOM of subsoil layers remains consistent with the wollastonite amendment. In line with our results, Haque et al. (2019) observed amendment with wollastonite increase and decrease the SIC and SOC content of soil through a pot experiment, respectively. In contrast, te Pas et al. (2023) did not observe any noticeable change in the SOC of soil due to wollastonite (and other silicate minerals) treatment.

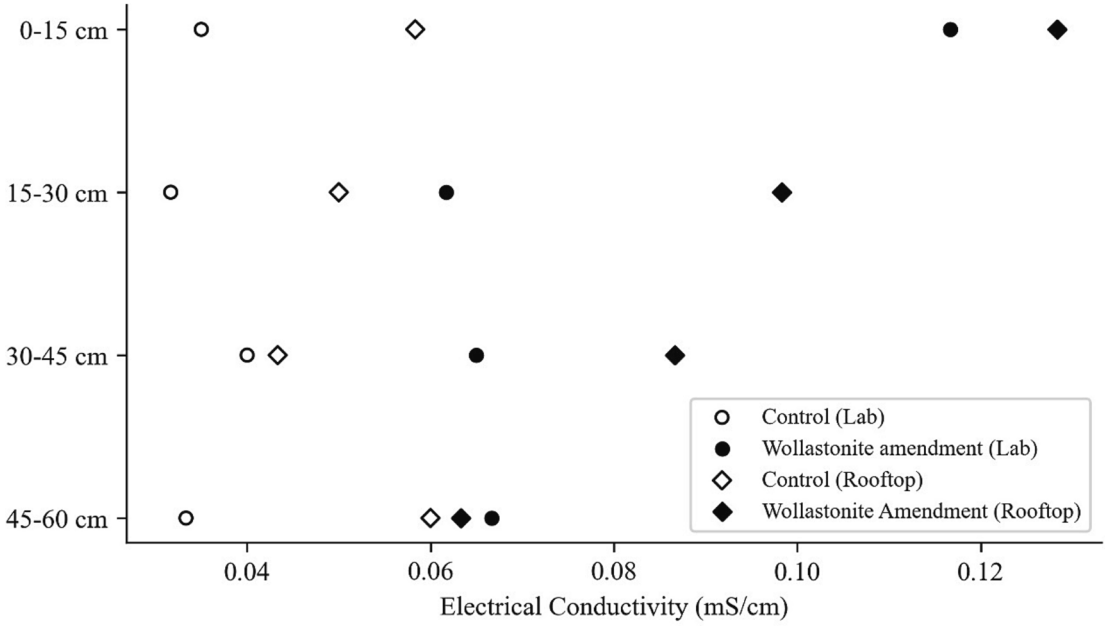

Fig. 4. Impact of wollastonite amendment on EC of different depths over the vertical profile of the soil. Error bars are smaller than the size of the symbols (all are in the range of $P < 0.05$).

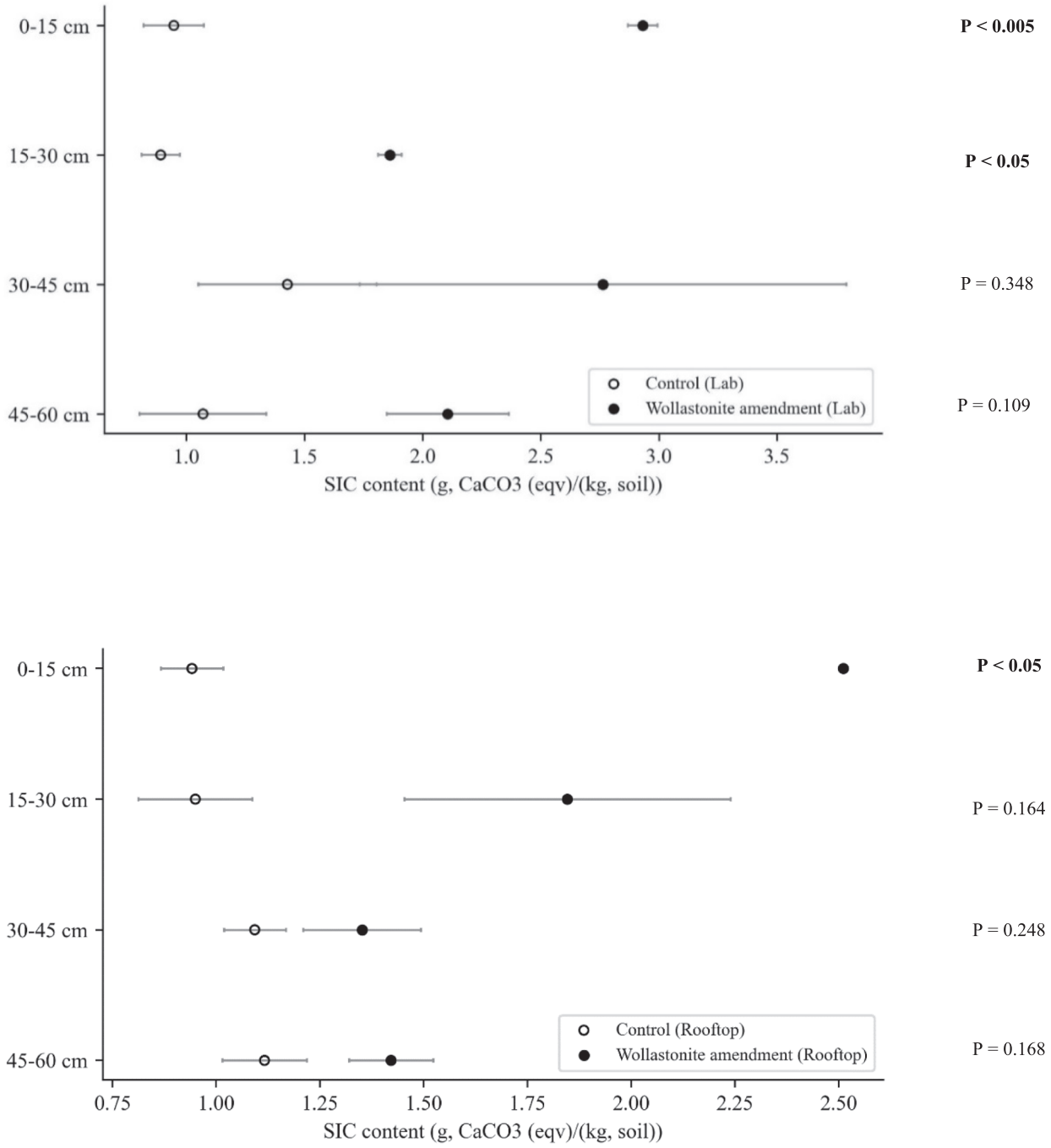

Fig. 5. The $CaCO_3$(eqv) content over the vertical horizon of soil in control and wollastonite amendments columns (above: Lab setup; below: Rooftop setup).

3.6. Carbon sequestration

To account for sequestrated carbon in the form of pedogenic carbonate, the difference between amended and control samples was determined. Then the sequestrated carbon in each column was determined considering the bulk density and depth of each layer as described in Khalidy et al. (2021). Accordingly, a net amount of 6.12 and 2.85 CO_2 t/ha was estimated to be sequestered in the form of pedogenic carbonate in the wollastonite amendment columns in Lab and Rooftop setups, respectively. Taking into consideration the dosage of applied wollastonite (50 t/ha), the efficiency of sequestration is expected to be 0.12 and 0.07 t CO_2 per tonne of applied wollastonite in Lab and Rooftop setups, respectively.

Considering the mass of Ca accumulated in the solid phase as pedogenic carbonate (Fig. 5) and the mass of Ca and Mg in the leachate effluent (Fig. 1) due to wollastonite amendment, and assuming that those leached ions are speciated primarily as bicarbonate considering the alkaline pH of the effluent (Fig. 1) and over the soil profile (Fig. 3), it is calculated that ratio of CO_2 drawdown in the form carbonate:bicarbonate is approximately 15:1. Therefore, the total amount of sequestrated carbon is 6.53 CO_2 t/ha in the Lab setup. Such a high ratio is attributed in this study to: the alkaline nature of the soil/subsoil system (pH range of 6.82 to 7.39, Fig. 3); the moderate rate of evapotranspiration when considering the leachate volume fraction compared to the

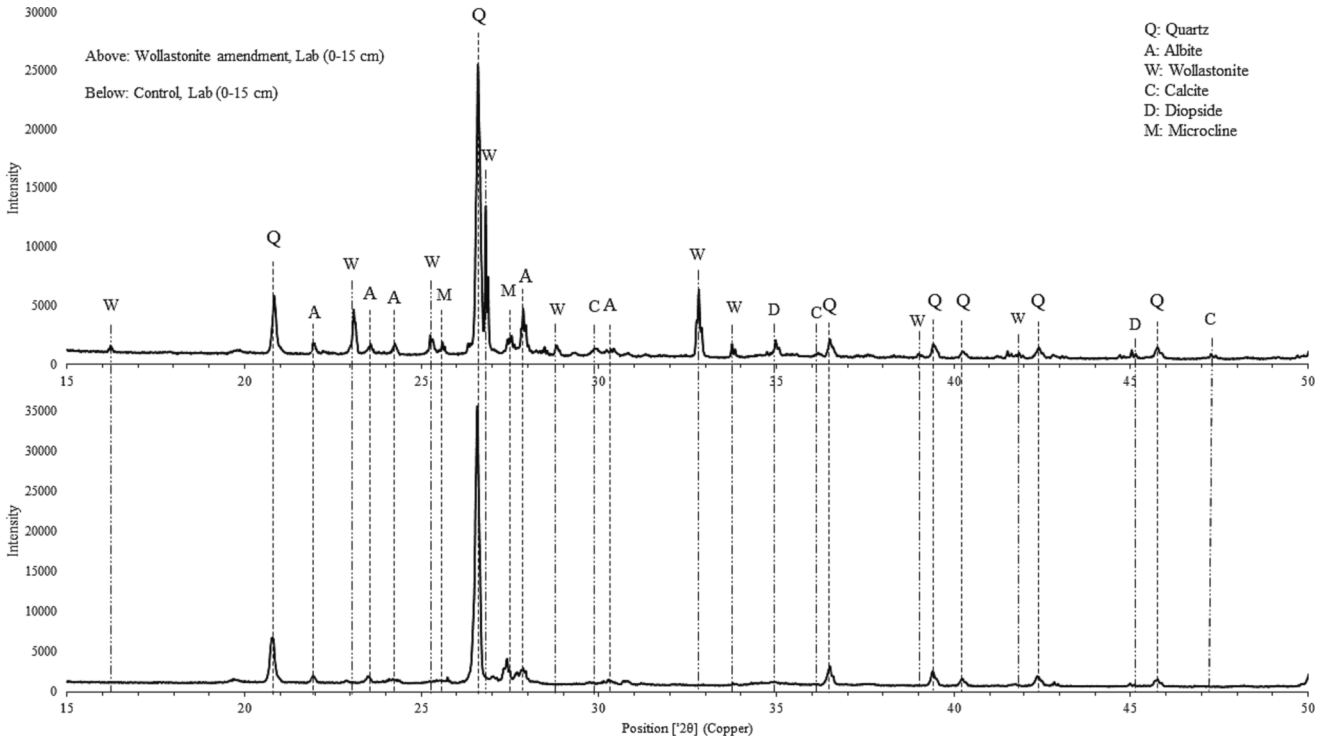

Fig. 6. XRD diffractograms of wollastonite amendment (above) and control (below) samples (0–15 cm layer, lab setup). Dash lines are representative of mineral phases present in both control and amended samples. While long-dash dotted lines highlight the weathering products in amended soil.

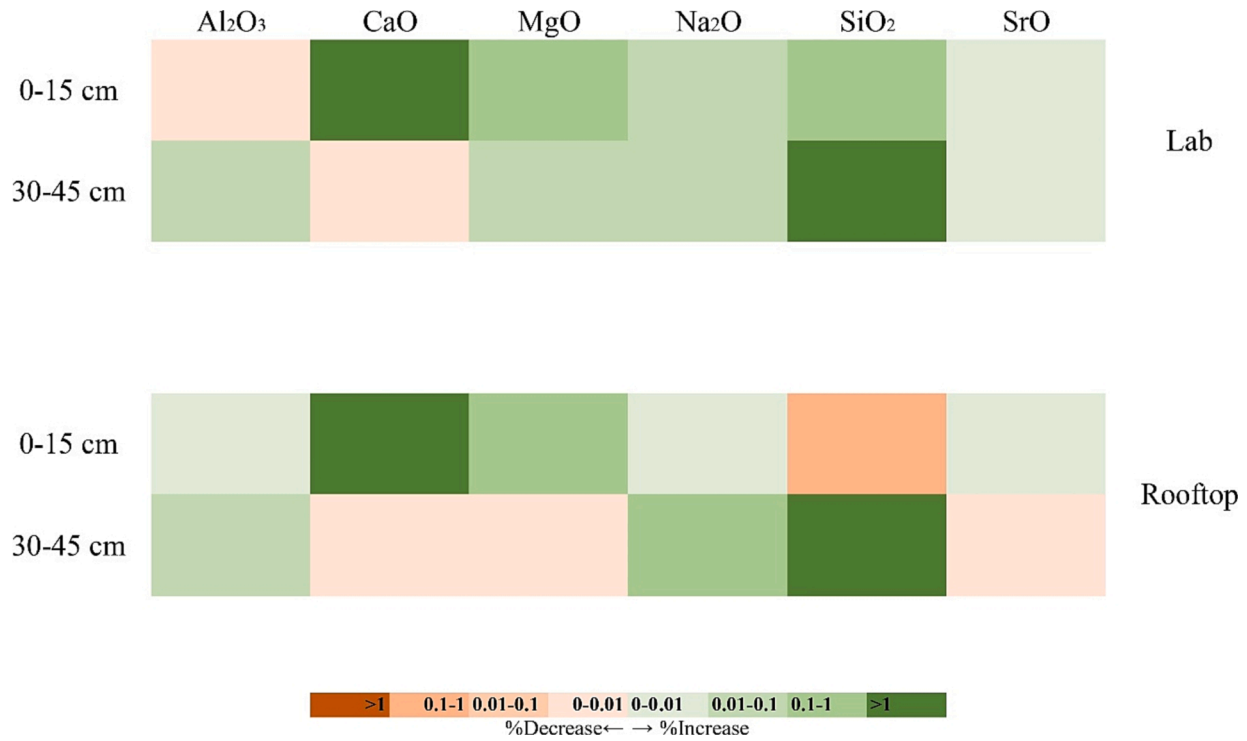

Fig. 7. Changes in the elemental composition (XRF) of soil samples after wollastonite amendment with reference to corresponding control composition.

irrigation volume (recovery ratio average of 0.864 ± 0.10 and 0.867 ± 0.09 for control and wollastonite Lab columns, respectively, but as low as 0.48 episodically); and the possibility that wollastonite grains carbonate homogeneously within the soil (i.e., on the surface of the mineral grains) as inferred in a prior study (Haque et al., 2020c).

In Fig. 9, the efficiency of sequestration in the present study is compared with data reported in the literature for wollastonite, basalt, and olivine (Amann et al., 2020; Haque et al., 2019; Kelland et al., 2020; Ten Berge et al., 2012; Vienne et al., 2022). The efficiency is plotted as a ratio of RCO_2, describing the maximum potential CDR based on CaO% and MgO% in the elemental composition of a silicate mineral (Renforth 2012). According to this image, olivine has the highest theoretical

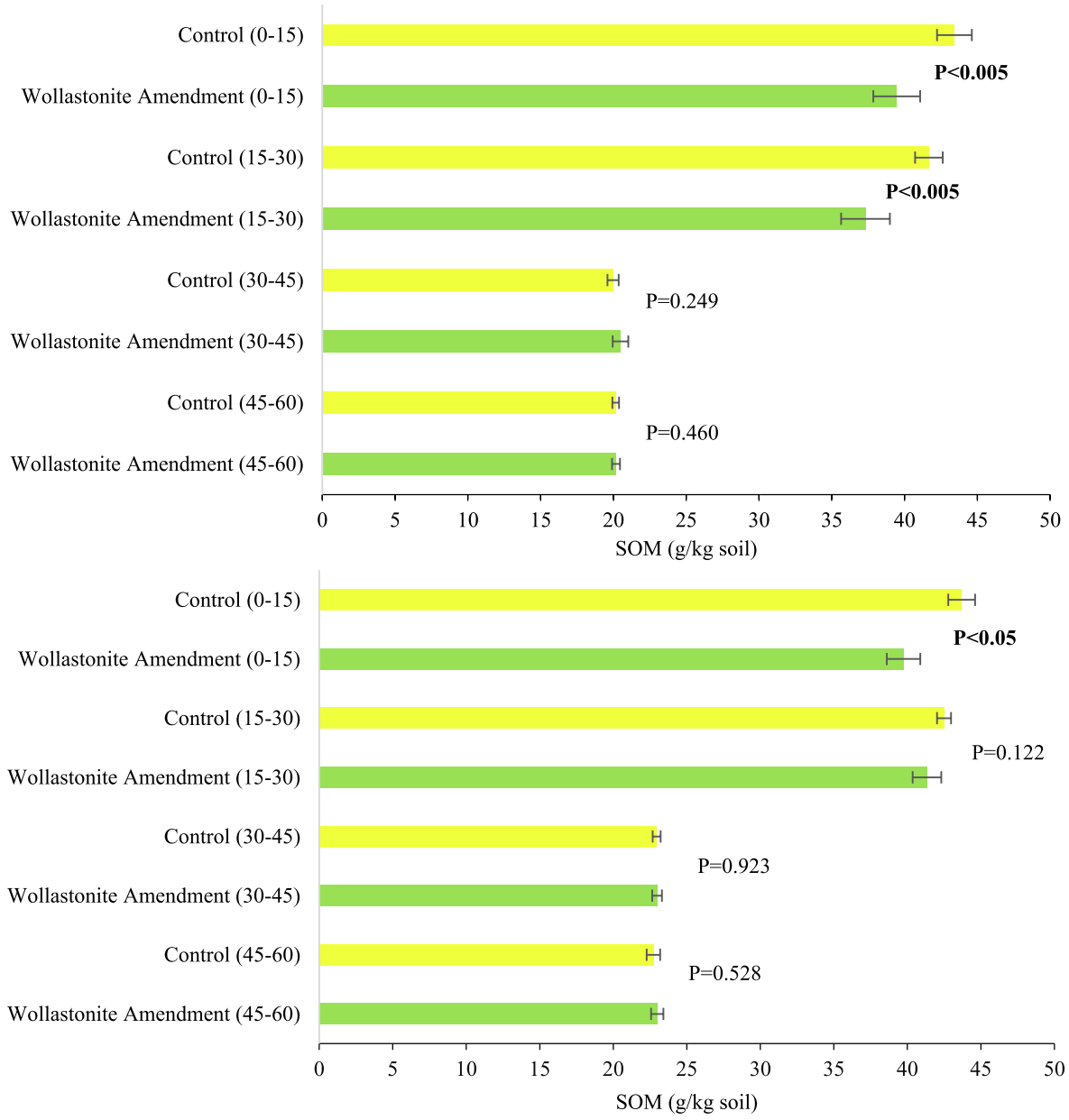

Fig. 8. The SOM content of different layers of control and wollastonite amendments columns (above: Lab setup; below: Rooftop setup). The SOM values of the wollastonite amended 0-15 cm layers were corrected for mineral dilution effect by a factor of 3 wt% (i.e., times 1.03).

potential, while wollastonite is the most robust in terms of efficiency. As implied from Table 1 and Figure.S1, the wollastonite ore used in this study contains diopside ($MgCaSi_2O_6$). This encouraged us to investigate three scenarios by considering (i) both CaO and MgO (ii) CaO, and (iii) net CaO excluding diopside as the possible sinks for carbon mineralization. This results in satisfying 42% (19%), 49% (23%), and 61% (28%) of maximum CDR potential in Lab (Rooftop) samples in the first, second, and third abovementioned scenarios, respectively.

3.7. Tracing weathering products; leachate vs. Solid form

As discussed in the previous section, wollastonite amendment gives rise to pedogenic carbonate (PC) formation over the soil profile and enhances the efflux of Ca and Mg in the leachate. To account for all these portions, the weathering rate of wollastonite attributed to released Ca accumulating in solid form as PC (Wr(Wol_Sol)) and attributed to Ca leaving the soil profile in the leachate form (Wr(Wol_Lea)), and the weathering rate of diopside attributed to Ca and Mg leaving the soil profile in the leachate form (Wr(Dio_Lea)) were considered, as illustrated in Fig. 10, where Wr(Total) represents the sum of all three portions. The Wr(Wol_Lea) was determined considering the net effluent flux of Ca, excluding Ca sourced from diopside. Details of the method for calculating each Wr value are provided in the Supplementary Material (Eqs. S3-S5)). The results reveal that Wr(Wol_Sol) ($3.2{\cdot}10^{-10}$ mol $Ca{\cdot}m^{-2}{\cdot}s^{-1}$, on average) is controlling the ERW process and is in the range of 10x to 1000x higher than weathering rates of wollastonite and diopside determined based on Ca and Mg detected in the leachate (Wr(Wol_Lea) and Wr(Dio_Lea)). The Wr of wollastonite attributed to the leachate (Wr(Wol_Lea) shows a declining trend, suggesting a considerable decline of wollastonite content in the column (also, such decline can be a sign of reducing surface area based on a shrinking particle analogy or even particle passivation) while the weathering rate of diopside (Wr(Dio_Lea)) is rather consistent over time, which is expected for a slower weathering mineral. It should be noted that oscillations in

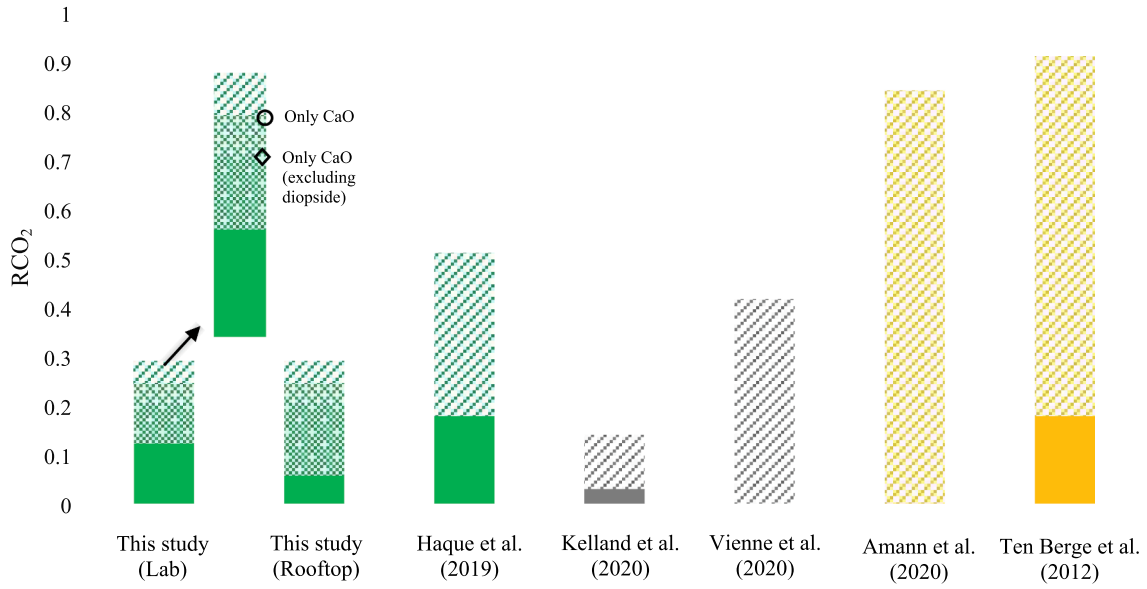

Fig. 9. Comparison of estimated CO_2 sequestration efficiency in ERW column experiments (the filled portion of bars represents the reported efficiency while the total bars represent the theoretical CDR potential of the applied silicate mineral). The green, grey, and orange colors represent wollastonite, basalt, and olivine applications, respectively. The normalized data of plotted studies are retrieved from the Kelland et al. (2020) article. Different shades in the leftmost bar are representative of different scenarios of (i) both CaO and MgO (ii) CaO, and (iii) net CaO excluding diopside (ordered from largest amount).Note only carbon drawdown in pedogenic carbonate is considered in the case of the present study. (For interpretation of the references to colour in this figure legend, the reader is referred to the web version of this article.)

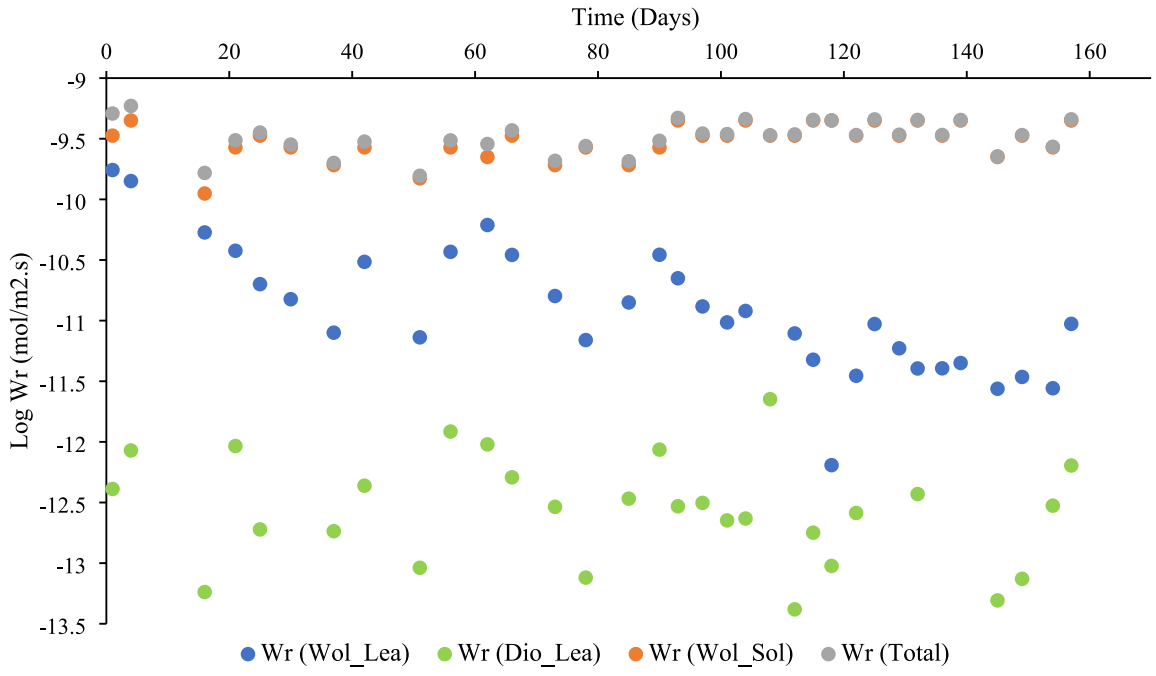

Fig. 10. The weathering rate (Wr, log (mol/m^2/s) of mineral, in terms of net pedogenic carbonate accumulation (Wr(Wol_Sol)), wollastonite in form of leachate (Wr (Wol_Lea)), and diopside in form of leachate (Wr(Dio_Lea)) over the duration of the experiment. The sum of the mentioned portions is displayed as the total value (Wr(Total)).

Fig. 10 are largely due to variations in water flux through the columns (i.e., residence time) and in evapotranspiration (i.e., water balance between input and leachate), but these oscillations do not significantly mask the weathering signals due to the relatively fast weathering rate of the minerals.

It is implicit that solely considering the leachate concentrations as the weathering signal significantly underestimates the Wr, and the omissions of the inclusion of PC determination may have resulted in underestimated Wr values in previous studies that have reported lower than expected Wr values for Mg-based silicate minerals such as basalt (Buckingham et al., 2022; Kelland et al., 2020) and olivine (Renforth et al., 2015). The measured total Wr (sum of Wr(Wol_Sol) and Wr (Wol_Lea)) for wollastonite (range of log Wr: −9.80 to −9.23 mol $Ca{\cdot}m^{-2}{\cdot}s^{-1}$) and diopside (range of log Wr: −13.38 to −11.64 mol $Mg{\cdot}m^{-2}{\cdot}s^{-1}$) in our study are comparable with values compiled by Palandri and Kharaka (2004) based on laboratory datasets (log Wr:

−9.04 (at 20° C) to −8.88 $Ca \cdot m^{-2} \cdot s^{-1}$ (at 25° C) and log Wr: −11.23 (at 20° C) to −11.11 $Mg \cdot m^{-2} \cdot s^{-1}$ (at 25° C) at pH greater than 6 for wollastonite and diopside, respectively). It can be implied that disregarding weathering products accumulated in the solid phase (e.g., pedogenic carbonate) and reporting solely weathering rate based on leachate products (as has been the case in other column/profile studies), can underestimate the weathering rate of silicate minerals. Especially for wollastonite and other Ca-rich silicate minerals, it is critical that ERW studies not disregard the PC pathway to CO_2 drawdown, even in short-term experiments. Some studies claim that their acidic soils are not conducive to PC accumulation, but that may not be the case in the subsoils under those acidic soils, or that Mg-carbonates are less likely to form in soils, but with strong evapotranspiration and soil drying, some Mg-carbonates are seen to form in natural systems subjected to drying-induced supersaturation, such as nesquehonite and hydromagnesite (Raudsepp et al., 2023).

Wollastonite treatment has a negligible impact on Ni and Cr levels of the column leachate (Fig. 1). This hints that wollastonite application on a field scale (which is reckoned to be much less than 50 t/ha used in the present study) will not have significant health hazard to the environment. In comparison, the dissolution of olivine is recognized as a potential carrier of Ni and Cr from soil solution in studies conducted by te Pas et al. (2023) and Amann et al. (2020).

Fig. 11 illustrates a summary of processes occurring throughout the experiment in the presence and absence of wollastonite. As discussed in the previous section, wollastonite amendment gives rise to PC formation over the soil profile. However, a large portion (39 ~ 51%) of wollastonite remains in other forms (weathered or unweathered) in the system. The results of XRD (Fig. 6 and Fig. S3) and XRF (Fig. 7) illustrate the presence of wollastonite in the soil of 0–15 cm layer of "wollastonite amendment" columns. Furthermore, the soil layers' pH, EC, and carbonate content analyses imply that wollastonite weathering in the Rooftop setup is significantly limited to top layers (e.g., 0–15 and 15–30 cm). Looking into climatic data (Fig. S4, acquired from the local station located on the rooftop of the School of Engineering, University of Guelph), the precipitation during the experiment was less than half of the normal rainfall of the region. This might also come with long dry interludes, causing ponding after heavy rainfall episodes and increasing evaporation. Comparing the Lab and Rooftop setups, the latter received almost three times less water during the experiment. This could restrict the weathering of minerals and percolating water to the deeper layers. Furthermore, the ambient temperature of the rooftop tends to decrease after September (Fig. S4), and a major part of the experiment was run in much less than the ambient temperature. Such low temperatures (daily average of 16.60, 9.94, and 4.69 °C for September, October, and November, respectively) slow down the dissolution of silicate minerals as pinpointed by Haque et al. (2023) and Pogge von Strandmann et al. (2022).

Exposure to natural climate (e.g., sunlight and rainfall) is accompanied by higher evapotranspiration rates. This leads to more rapid drying of the topsoil and greater absorption of the majority of the percolating water lower within the column by soil particles; hence, the leachate will be very limited as observed in both the rooftop setups of the present study and that of Buckingham et al. (2022). As evapotranspiration will promote a cycle of weathering followed by solution saturation and carbonate precipitation, focusing solely on Wr due to water flow leads to an underestimation of the weathering rate in this condition. As pointed out by West et al. (2023), soil analyses (e.g., calcimetry, XRD analysis, and elemental analysis) should be taken into account in this type of experiment to monitor the progression of weathering and carbon drawdown. Moreover, it is critical to understand that results from mesocosm experiments conducted under higher rates of evapotranspiration can be informative to predict ERW behavior in hotter and drier climates, so it should be expected that the monitoring methods to track ERW are not necessarily the same in every global region.

4. Conclusion

To investigate the fate of weathering products due to wollastonite skarn addition over the vertical profile of soil, under varied irrigation and water percolation regimes that represented wetter and drier and less variable and more variable temperature regimes, we developed a soil

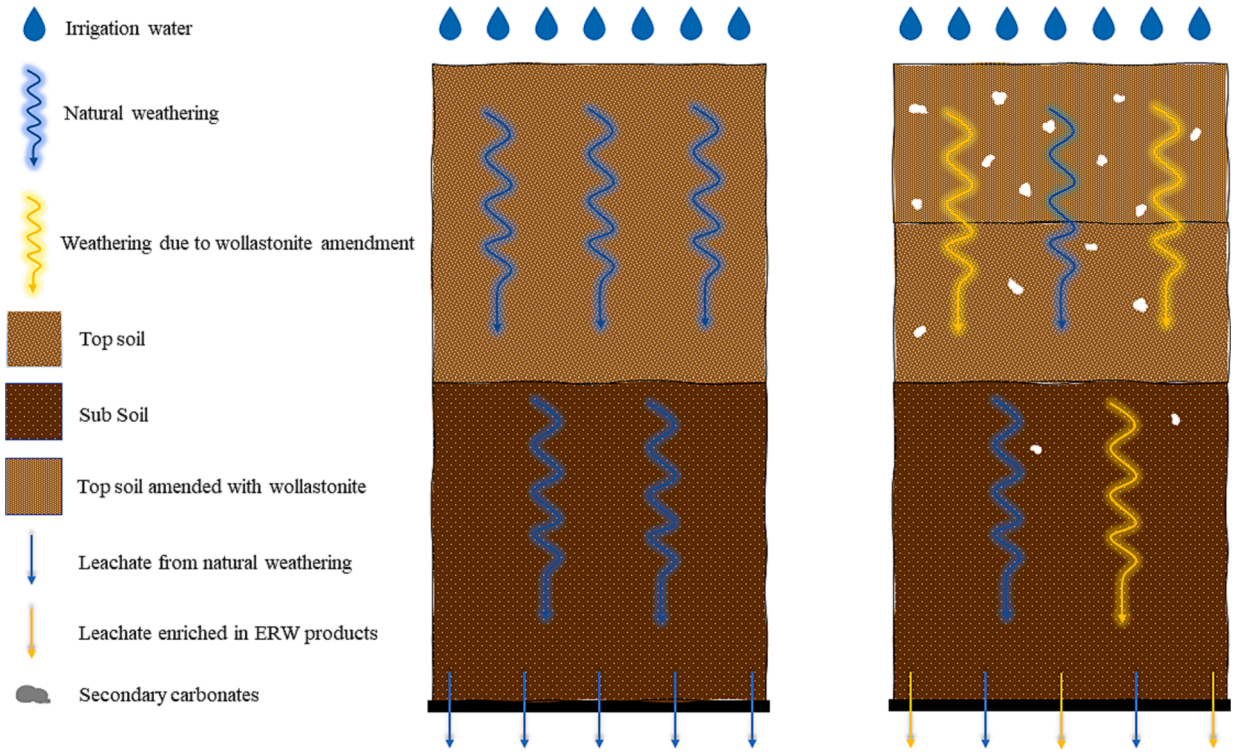

Fig. 11. Illustration of processes affecting weathering with (right) and without (left) wollastonite amendment in the experimental setup.

column experiment buildup of distinct layers of topsoil and subsoil in the laboratory and natural (rooftop) settings. The results showed that the effect of wollastonite treatment is significantly evident on the geochemistry of topsoil layers (0–15 and 15–30 cm), while the lowest alteration was observed in the subsoil of the Rooftop setup. We estimated carbon sequestration of 6.53 and 2.85 tCO_2/ha as (pedogenic carbonate) in Lab and Rooftop setups, respectively. The disparity between the effect of wollastonite on the Lab and Rooftop setups was attributed to diverse climatic and ambient conditions. This includes the lower quantity of water (in the form of rainfall) received by Rooftop columns and lower ambient temperature in the Fall compared to a temperature-controlled Lab setup. Our observations revealed wollastonite is capable of modifying the solid phase of soil over a few months, in contrast to other silicate minerals examined in previous studies. Based on our calculation, Wr estimated from the formation of pedogenic carbonate is significantly higher compared to Wr measured from leachate efflux, and therefore both of these portions of CO_2 drawdown should be considered in ERW studies, particularly those using Ca-rich minerals, neutral-to-alkaline soils or having more alkaline subsoils despite an acidic topsoil, and where the rate of evapotranspiration is high leading to oscillations in soil saturation and thus in carbonate supersaturation, in order to avoid underestimation of silicate minerals weathering rates. The results of our study spotlight the key role of water flow in the dissolution and migration of weathering products during enhanced rock weathering practice. Understanding the fate of ERW products over the soil horizon is important for achieving an accurate estimation of carbon sequestration efficiency. This type of evaluation is deemed as an emboldening step of ERW practice prior to the transition to a global-scale carbon sequestration approach.

Declaration of Competing Interest

The authors declare that they have no known competing financial interests or personal relationships that could have appeared to influence the work reported in this paper.

Data availability

Data will be made available on request.

Acknowledgments

This research was funded by the Ontario Agri-Food Innovation Alliance (Gryphon's LAAIR Product Development grant UG-GLPD-2021-101200), the Natural Sciences and Engineering Research Council of Canada (Discovery Grant 401497), and the Ministry of Colleges and Universities (Early Researcher Awards). The authors would like to thank graduate students (Jinghan Zhao, Hiral Jariwala, and Leonardo Gadelha) and lab technicians (Michael Speagle and Ken Graham) of the School of Engineering, University of Guelph, for their help in building and running the experimental setups of this study.

Appendix A. Supplementary material

Supplementary data to this article can be found online at https://doi.org/10.1016/j.catena.2023.107524.

References

Amann, T., Hartmann, J., 2022. Carbon Accounting for Enhanced Weathering. Front. Clim. 4, 849948 https://doi.org/10.3389/fclim.2022.849948.

Amann, T., Hartmann, J., Struyf, E., de Oliveira Garcia, W., Fischer, E.K., Janssens, I.A., Meire, P.M., Schoelynck, J., 2020. Enhanced Weathering and related element fluxes-A cropland mesocosm approach. Biogeosciences 17, 103–119. https://doi.org/10.5194/bg-17-103-2020.

Andrews, M.G., Taylor, L.L., 2019. Combating Climate Change Through Enhanced Weathering of Agricultural Soils. Elements 15, 253–258. https://doi.org/10.2138/gselements.15.4.253.

Balestrini, R., Galli, L., Tartari, G., 2000. Wet and dry atmospheric deposition at prealpine and alpine sites in northern Italy. Atmos. Environ. 34, 1455–1470. https://doi.org/10.1016/S1352-2310(99)00404-5.

Barton, C.D., Karathanasis, A.D., Chalfant, G., 2002. Influence of acidic atmospheric deposition on soil solution composition in the Daniel Boone National Forest, Kentucky. USA. Environ. Geol. 41, 672–682. https://doi.org/10.1007/s00254-001-0450-6.

Beerling, D.J., Leake, J.R., Long, S.P., Scholes, J.D., Ton, J., Nelson, P.N., Bird, M., Kantzas, E., Taylor, L.L., Sarkar, B., Kelland, M., DeLucia, E., Kantola, I., Müller, C., Rau, G., Hansen, J., 2018. Farming with crops and rocks to address global climate, food and soil security. Nat. Plants 4, 138–147. https://doi.org/10.1038/s41477-018-0108-y.

Buckingham, F.L., Henderson, G.M., Holdship, P., Renforth, P., 2022. Soil core study indicates limited CO_2 removal by enhanced weathering in dry croplands in the UK. Appl. Geochemistry 147, 105482. https://doi.org/10.1016/j.apgeochem.2022.105482.

Dupla, X., Möller, B., Baveye, P.C., Grand, S., 2023. Potential accumulation of toxic trace elements in soils during enhanced rock weathering. Eur. J. Soil Sci. 74, e13343.

Goll, D.S., Ciais, P., Amann, T., Buermann, W., Chang, J., Eker, S., Hartmann, J., Janssens, I., Li, W., Obersteiner, M., Penuelas, J., Tanaka, K., Vicca, S., 2021. Potential CO_2 removal from enhanced weathering by ecosystem responses to powdered rock. Nat. Geosci. 14, 545–549. https://doi.org/10.1038/s41561-021-00798-x.

Gu, X., Fang, X., Xiang, W., Zeng, Y., Zhang, S., Lei, P., Peng, C., Kuzyakov, Y., 2019. Vegetation restoration stimulates soil carbon sequestration and stabilization in a subtropical area of southern China. Catena 181, 104098. https://doi.org/10.1016/j.catena.2019.104098.

Haque, F., Chiang, Y.W., Santos, R.M., 2020a. Risk assessment of Ni, Cr, and Si release from alkaline minerals during enhanced weathering. Open Agric. 5, 166–175. https://doi.org/10.1515/opag-2020-0016.

Government of Canada, 2023. Historical Climate Data. https://climate.weather.gc.ca/index_e.html. (Accessed on 10/06/2023).

Haque, F., Khalidy, R., Chiang, Y.W., Santos, R.M., 2023. Constraining the Capacity of Global Croplands to CO_2 Drawdown via Mineral Weathering. ACS Earth Space Chem., in press. 10.1021/acsearthspacechem.2c00374.

Haque, F., Santos, R.M., Dutta, A., Thimmanagari, M., Chiang, Y.W., 2019. Co-Benefits of Wollastonite Weathering in Agriculture: CO_2 Sequestration and Promoted Plant Growth. ACS Omega 4, 1425–1433. https://doi.org/10.1021/acsomega.8b02477.

Haque, F., Santos, R.M., Chiang, Y.W., 2020b. CO_2 sequestration by wollastonite-amended agricultural soils–An Ontario field study. Int. J. Greenh. Gas Control 97, 103017. https://doi.org/10.1016/j.ijggc.2020.103017.

Haque, F., Santos, R.M., Chiang, Y.W., 2020c. Optimizing Inorganic Carbon Sequestration and Crop Yield With Wollastonite Soil Amendment in a Microplot Study. Front. Plant Sci. 11, 1012. https://doi.org/10.3389/fpls.2020.01012.

Hartmann, J., West, A.J., Renforth, P., Köhler, P., De La Rocha, Wolf-Gladrow, D.A., Dürr, H.H., Scheffran, J., 2013. Enhanced chemical weathering as a geoengineering strategy to reduce atmospheric carbon dioxide, supply nutrients, and mitigate ocean acidification. Rev. Geophys. 51, 113–149. https://doi.org/10.1002/rog.20004.

Howard, P.J.A., Howard, D.M., 1990. Use of organic carbon and loss-on-ignition to estimate soil organic matter in different soil types and horizons. Biol. Fertil. Soils 9, 306–310. https://doi.org/10.1007/BF00634106.

Jariwala, H., Haque, F., Vanderburgt, S., Santos, R.M., Chiang, Y.W., 2022. Mineral–Soil–Plant–Nutrient Synergisms of Enhanced Weathering for Agriculture: Short-Term Investigations Using Fast-Weathering Wollastonite Skarn. Front. Plant Sci. 13, 929457 https://doi.org/10.3389/fpls.2022.929457.

Jorat, M.E., Goddard, M.A., Manning, P., Kwan, H., Ngeow, S., Sohi, S.P., Manning, D.A.C., 2020. Passive CO_2 removal in urban soils : Evidence from brownfield sites. Sci. Total Environ. 703, 135573 https://doi.org/10.1016/j.scitotenv.2019.135573.

Jorat, M.E., Kraavi, K.E., Manning, D.A.C., 2022. Removal of atmospheric CO_2 by engineered soils in infrastructure projects. J. Environ. Manage. 314, 115016 https://doi.org/10.1016/j.jenvman.2022.115016.

Kantola, I.B., Masters, M.D., Beerling, D.J., Long, S.P., DeLucia, E.H., 2017. Potential of global croplands and bioenergy crops for climate change mitigation through deployment for enhanced weathering. Biol. Lett. 13, 20160714. https://doi.org/10.1098/rsbl.2016.0714.

Kantzas, E.P., Val Martin, M., Lomas, M.R., Eufrasio, R.M., Renforth, P., Lewis, A.L., Taylor, L.L., Mecure, J.F., Pollitt, H., Vercoulen, P.V., Vakilifard, N., Holden, P.B., Edwards, N.R., Koh, L., Pidgeon, N.F., Banwart, S.A., Beerling, D.J., 2022. Substantial carbon drawdown potential from enhanced rock weathering in the United Kingdom. Nat. Geosci. 15, 382–389. https://doi.org/10.1038/s41561-022-00925-2.

Kelemen, P.B., McQueen, N., Wilcox, J., Renforth, P., Dipple, G., Vankeuren, A.P., 2020. Engineered carbon mineralization in ultramafic rocks for CO_2 removal from air: Review and new insights. Chem. Geol. 550, 119628 https://doi.org/10.1016/j.chemgeo.2020.119628.

Kelland, M.E., Wade, P.W., Lewis, A.L., Taylor, L.L., Sarkar, B., Andrews, M.G., Lomas, M.R., Cotton, T.E.A., Kemp, S.J., James, R.H., 2020. Increased yield and CO_2 sequestration potential with the C_4 cereal *Sorghum bicolor* cultivated in basaltic rock dust-amended agricultural soil. Glob. Chang. Biol. 26, 3658–3676. https://doi.org/10.1111/gcb.15089.

Khalidy, R., Santos, R.M., 2021b. Assessment of geochemical modeling applications and research hot spots—a year in review. Environ. Geochem. Health 43, 3351–3374. https://doi.org/10.1007/s10653-021-00862-w.

Khalidy, R., Haque, F., Chiang, Y.W., Santos, R.M., 2021. Monitoring Pedogenic Inorganic Carbon Accumulation Due to Weathering of Amended Silicate Minerals in Agricultural Soils. J. Vis. Exp. 172, e61996.

Khalidy, R., Arnaud, E., Santos, R.M., 2022. Natural and Human-Induced Factors on the Accumulation and Migration of Pedogenic Carbonate in Soil: A Review. Land 11, 1448. https://doi.org/10.3390/land11091448.

Khalidy, R., Santos, R.M., 2021a. The fate of atmospheric carbon sequestrated through weathering in mine tailings. Miner. Eng. 163, 106767 https://doi.org/10.1016/j.mineng.2020.106767.

La Plante, E.C., Mehdipour, I., Shortt, I., Yang, K., Simonetti, D., Bauchy, M., Sant, G.N., 2021. Controls on CO_2 Mineralization Using Natural and Industrial Alkaline Solids under Ambient Conditions. ACS Sustain. Chem. Eng. 9, 10727–10739. https://doi.org/10.1021/acssuschemeng.1c00838.

Lefebvre, D., Goglio, P., Williams, A., Manning, D.A.C., de Azevedo, A.C., Bergmann, M., Meersmans, J., Smith, P., 2019. Assessing the potential of soil carbonation and enhanced weathering through Life Cycle Assessment: A case study for Sao Paulo State. Brazil. J. Clean. Prod. 233, 468–481. https://doi.org/10.1016/j.jclepro.2019.06.099.

Lindsey, R., Dahlman, L., 2020. Climate change: Global temperature. https://www.climate.gov/news-features/understanding-climate/climate-change-global-temperature (Accessed 10/06/2023).

Manning, D.A.C., Renforth, P., Lopez-Capel, E., Robertson, S., Ghazireh, N., 2013. Carbonate precipitation in artificial soils produced from basaltic quarry fines and composts: An opportunity for passive carbon sequestration. Int. J. Greenh. Gas Control 17, 309–317. https://doi.org/10.1016/j.ijggc.2013.05.012.

Moosdorf, N., Renforth, P., Hartmann, J., 2014. Carbon Dioxide Efficiency of Terrestrial Enhanced Weathering. Environ. Sci. Tech. 48, 4809–4816. https://doi.org/10.1021/es4052022.

Palandri, J.L., Kharaka, Y.K., 2004. A compilation of rate parameters of water-mineral interaction kinetics for application to geochemical modeling. USGS Open File Rep. 2004–1068, 71.

Pogge von Strandmann, P.A.E., Tooley, C., Mulders, J.J.P.A., Renforth, P., 2022. The Dissolution of Olivine Added to Soil at 4°C: Implications for Enhanced Weathering in Cold Regions. Front. Clim. 4, 827698 https://doi.org/10.3389/fclim.2022.827698.

Rahmanihanzaki, M., Hemmati, A., 2022. A review of mineral carbonation by alkaline solidwaste. Int. J. Greenh. Gas Control 121, 103798. https://doi.org/10.1016/j.ijggc.2022.103798.

Raudsepp, M.J., Wilson, S., Morgan, B., 2023. Making Salt from Water: The Unique Mineralogy of Alkaline Lakes. Elements 19 (1), 22–29. https://doi.org/10.2138/gselements.19.1.22.

Rayment, G.E., Higginson, F.R., 1992. Australian laboratory handbook of soil and water chemical methods. Inkata Press Pty Ltd.

Renforth, P., 2012. The potential of enhanced weathering in the UK. Int. J. Greenh. Gas Control 10, 229–243. https://doi.org/10.1016/j.ijggc.2012.06.011.

Renforth, P., Pogge von Strandmann, P.A.E., Henderson, G.M., 2015. The dissolution of olivine added to soil: Implications for enhanced weathering. Appl. Geochemistry 61, 109–118. https://doi.org/10.1016/j.apgeochem.2015.05.016.

Ruiz Sinoga, J.D., Pariente, S., Diaz, A.R., Martinez Murillo, J.F., 2012. Variability of relationships between soil organic carbon and some soil properties in Mediterranean rangelands under different climatic conditions (South of Spain). Catena 94, 17–25. https://doi.org/10.1016/j.catena.2011.06.004.

Sanna, A., Uibu, M., Caramanna, G., Kuusik, R., Maroto-Valer, M.M., 2014. A review of mineral carbonation technologies to sequester CO_2. Chem. Soc. Rev. 43, 8049–8080. https://doi.org/10.1039/C4CS00035H.

Santos, R.M., Araujo, F., Jariwala, H., Khalidy, R., Haque, F., Chiang, Y.W., 2023. Pathways, roundabouts, roadblocks and shortcuts to safe and sustainable deployment of enhanced rock weathering in agriculture. Front. Earth Sci. 11, 1215930. https://doi.org/10.3389/feart.2023.1215930.

te Pas, E.E.E.M., Hagens, M., Comans, R.N.J., 2023. Assessment of the enhanced weathering potential of different silicate minerals to improve soil quality and sequester CO_2. Front. Clim. 4, 954064 https://doi.org/10.3389/fclim.2022.954064.

Ten Berge, H.F.M., Van der Meer, H.G., Steenhuizen, J.W., Goedhart, P.W., Knops, P., Verhagen, J., 2012. Olivine weathering in soil, and its effects on growth and nutrient uptake in ryegrass (*Lolium perenne* L.): a pot experiment. PLoS One 7, e42098.

Vienne, A., Poblador, S., Portillo-Estrada, M., Hartmann, J., Ijiehon, S., Wade, P., Vicca, S., 2022. Enhanced Weathering Using Basalt Rock Powder: Carbon Sequestration, Co-benefits and Risks in a Mesocosm Study With Solanum tuberosum. Front. Clim. 4, 869456 https://doi.org/10.3389/fclim.2022.869456.

Washbourne, C.L., Renforth, P., Manning, D.A.C., 2012. Investigating carbonate formation in urban soils as a method for capture and storage of atmospheric carbon. Sci. Total Environ. 431, 166–175. https://doi.org/10.1016/j.scitotenv.2012.05.037.

West, L.J., Banwart, S.A., Martin, M.V., Kantzas, E., Beerling, D.J., 2023. Making mistakes in estimating the CO_2 sequestration potential of UK croplands with enhanced weathering. Appl. Geochemistry 147, 105482. https://doi.org/10.1016/j.apgeochem.2023.105591.

Wu, L., Zhang, S., Ma, R., Chen, M., Wei, W., Ding, X., 2021. Carbon sequestration under different organic amendments in saline-alkaline soils. Catena 196, 104882. https://doi.org/10.1016/j.catena.2020.104882.

Yan, Y., Dong, X., Li, R., Zhang, Y., Yan, S., Guan, X., Yang, Q., Chen, L., Fang, Y., Zhang, W., Wang, S., 2023. Wollastonite addition stimulates soil organic carbon mineralization: evidences from 12 land-use types in subtropical China. Catena 225, 107031. https://doi.org/10.1016/j.catena.2023.107031.